Eur. Phys. J. B (2013) 86: 31
DOI: 10.1140/epjb/e2012-30629-5

THE EUROPEAN PHYSICAL JOURNAL B

Regular Article

# Distinguishability of stacks in ZnTe/ZnSe quantum dots via spectral analysis of Aharonov-Bohm oscillations*

Bidisha Roy[1,2,a], Haojie Ji[1,2], Siddharth Dhomkar[1,2], Fred J. Cadieu[1,2], Le Peng[2,3], Richard Moug[3], Maria C. Tamargo[2,3], and Igor L. Kuskovsky[1,2,b]

[1] Department of Physics, Queens College of CUNY, Flushing, NY-11367, USA
[2] The Graduate Center of CUNY, New York, NY-10016, USA
[3] Department of Chemistry, The City College of CUNY, New York, NY-10031, USA

Received 17 July 2012 / Received in final form 6 October 2012
Published online 4 February 2013 – 

**Abstract.** A spectral analysis of the Aharonov-Bohm (AB) oscillations in photoluminescence intensity was performed for stacked type-II ZnTe/ZnSe quantum dots (QDs) fabricated within multilayered Zn-Se-Te system with sub-monolayer insertions of Te. Robust AB oscillations allowed for fine probing of distinguishable QDs stacks within the ensemble of QDs. The AB transition magnetic field, $B_{AB}$, changed from the lower energy side to the higher energy side of the PL spectra revealing the presence of different sets of QDs stacks. The change occurs within the spectral range, where the contributing green and blue bands of the spectra overlapped. "Bundling" in lifetime measurements is seen at transition spectral regions confirming the results.

## 1 Introduction

The Aharonov-Bohm (AB) effect [1] is purely quantum mechanical phenomenon, due to a geometrical phase [2] arising from spatial coherence of the wave function; a charged particle moving in magnetic-field-free regions on a closed trajectory enclosing a magnetic flux can acquire a topological phase due to the interaction with the vector potential even though no classical Lorentz forces are present. Theoretically [3,4] it was predicted that the AB effect can also be observed for a dipole, a nominally neutral quasi-particle, via optical emission of radially polarized excitons in quantum rings (QR) and disk-like type-II quantum dots (QDs) – this so-called excitonic AB effect requires a ring-like topology of the system. The observation of AB effect signatures in QR [5] and type-II QDs [6,7] inspired greater interest in this field, including the possibility of AB exciton storage and manipulation via application of applied in-plane electric field [8]; recently, experimental observation of effects of the built-in electric field on the AB interference has been reported [9]. With the progress in nanoscale fabrication techniques, realizing advanced goals in quantum information applications by controlling of light and excitons can be possible via manipulation of AB excitons.

The optical manifestation of the AB effect has been observed in terms of the oscillation in excitonic energy [5,7] and the photoluminescence (PL) intensity [6,9–11]; reports on excitonic AB effect are more widely available for quantum ring systems (e.g. [5,8,9,12–15] and references therein), while relatively few are offered for type-II QDs [6,7,11,16,17]. In this work, we present a spectral analysis of the AB oscillations observed for photoluminescence (PL) intensity as a function of magnetic field to achieve fine probing of information related to lateral extent of excitons in stacked type-II ZnTe/ZnSe QDs. The findings are also supported by results of conventional cw- and time-resolved PL (TRPL) measurements.

## 2 Experimental

We study QDs formed via three submonolayer deposition cycles of Zn-Te-Zn sandwiched between nominally undoped ZnSe barriers in multilayered Zn-Se-Te samples grown via migration enhanced epitaxy. Growth details are given in references [18,19] and references therein.

High resolution PL measurements were performed by exciting the samples with the 351 nm line of a Coherent Innova 90C FreD Ar-ion laser, while the emission was detected by a thermoelectrically cooled CCD camera attached to a TriVista SP2 500i Triple monochromator. The magneto-PL experiments were performed in the Faraday geometry with a Janis Research 9 T superconducting magnet outfitted with fiber optic probes, used to excite and collect the PL. The detection for magneto-PL experiments was done by a portable high resolution Ocean Optics solid

* Contribution to the Topical Issue "Excitonic Processes in Condensed Matter, Nanostructured and Molecular Materials", edited by Maria Antonietta Loi, Jasper Knoester and Paul H. M. van Loosdrecht.

[a] e-mail: bidishae@gmail.com
[b] e-mail: Igor.Kuskovsky@qc.cuny.edu

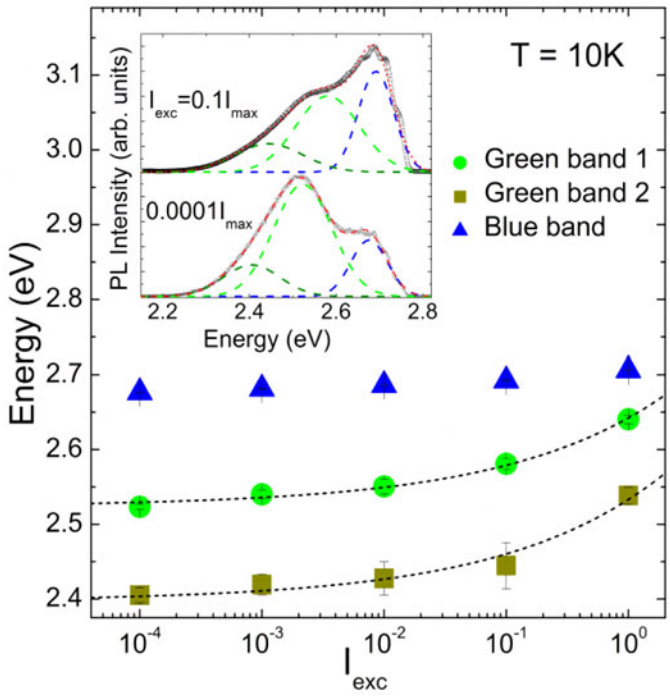


**Fig. 1.** (Color online) Plot of PL "green" and "blue" PL peaks (as shown in the inset) as a function of excitation intensity ($I_{exc}$); dashed line is the result of fitting with $I_{exc}^{1/3}$. Inset: low temperature (10 K) PL at two different ($I_{exc}$). The spectrum is decomposed into three Gaussian peaks.

state spectrometer. Time-resolved PL (TRPL) measurements were performed using the 337 nm line of a $N_2$ pulsed laser with 4 ns pulse width. The signal was recorded using a 500 MHz Tektronix TDS 654C oscilloscope. A Janis Research closed cycle refrigerating system was used for low temperature in both cw- and time-resolved PL measurements.

## 3 Results and discussions

### 3.1 Photoluminescence studies

The PL at 10 K is shown for two different excitation intensities ($I_{exc}$) in the inset of Figure 1. Three Gaussian peaks were used to decompose the PL spectrum; the "green" band is formed by two Gaussians ("Green band 1" at ∼2.52 eV and "Green band 2" at ∼2.4 eV) while the third Gaussian represents the "blue" band at ∼2.67 eV. As reported previously [19–22], in these systems, the PL of the QDs (generally seen as "green bands" at ∼2.5 eV and as low as 2.3 eV [19,23]) is convoluted with the emission from excitons bound to isoelectronic centers (ICs) of various sizes ($Te_{n\geqslant 2}$) (generally seen as "blue band" at ∼2.6 eV and higher energy shoulders).

The excitation intensity dependence of each of the three decomposed Gaussian peaks is shown in Figure 1. The "Green" bands 1 and 2 exhibit large shift (∼116 meV and ∼133 meV, respectively) when $I_{exc}$ is varied over four orders of magnitude. Such a shift that closely follows the cube root of excitation intensity (fitted by dashed lines in Fig. 1) is a signature of type-II band alignment in quantum structures ([20,21] and references therein). The IC-bound exciton dominated "blue" band shows a relatively smaller shift of ∼31 meV, which may be related to its significant overlap with the QD- related band. Evidently, with decreasing the excitation intensity, the QD PL starts to dominate, as the IC-related transitions are suppressed.

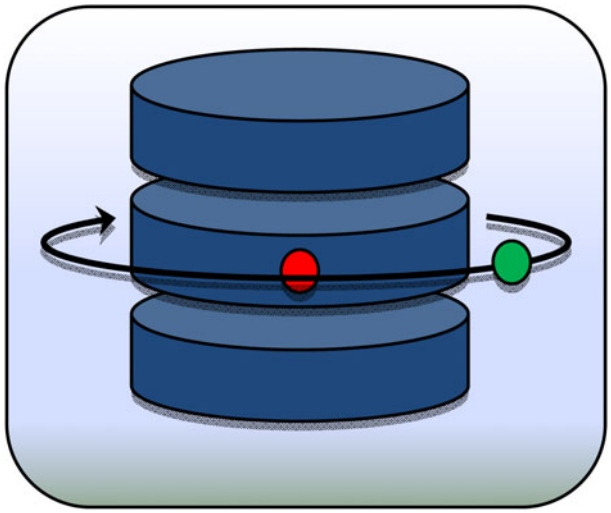

**Fig. 2.** (Color online) A schematic showing the model of stacked ZnTe rich disks where in the hole is strongly confined and electron (in ZnSe barrier) orbiting around the whole stack.

### 3.2 Magneto-PL studies: AB oscillations in PL emission intensity

#### 3.2.1 Integrated intensity

The AB phase can reveal itself in magneto-PL of cylindrical type-II QDs via the change of the exciton ground state ($|L = 0\rangle$) to a non-zero orbital angular momentum state with increasing magnetic field (flux) [4]. This transition of the angular momentum to a non-zero value can be observed as an oscillation in the PL intensity due to relaxed optical selection rules – caused by anisotropy, e.g. elongation, presence of impurities, and/or built-in electric field [6,9,11]. Also the "peak" in magneto-PL of disk-like type-II QDs (one carrier is confined within the dot), appears in real experiments where the whole system is in the magnetic field, the electron (hole) wavefunction is "squeezed" closer to the QD boundary [24], leading to an increase in the electron-hole overlap, and thus increased PL intensity, which abruptly decreases when the electron (hole) changes its state from $|L = 0\rangle$ to $|L \neq 0\rangle$ with increasing magnetic flux (field).

Our samples can be described by a model considered in reference [6]; the samples are stacks of multiple ZnTe-rich disks, containing strongly confined holes, while the electrons are located in the ZnSe barriers (Fig. 2 shows a schematic of the model). It is assumed that not all QDs

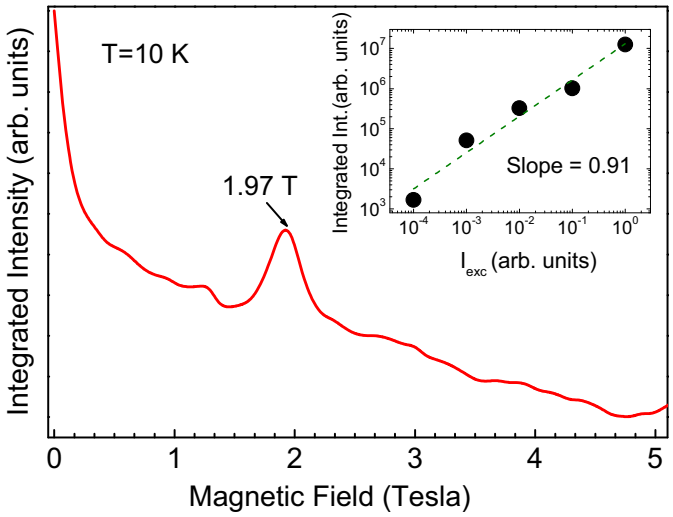


**Fig. 3.** (Color online) Integrated PL intensity as a function of magnetic field; the AB oscillation is at $B_{AB} = 1.97$ T. Inset: almost linear (dashed line) behavior of the integrated PL intensity as a function of $I_{exc}$.

are occupied by holes, and electrons move around a whole stack attracted by Coulomb interaction with the holes across the barriers. Such a configuration averages out the QD size variation and ensures cylindrical symmetry, which is ideal for the observation of AB effect.

Figure 3 shows integrated PL intensity as a function of applied magnetic field. AB oscillation is seen at a transition magnetic field, $B_{AB} \approx 1.97$ T. The observation of the robust AB oscillation (magnitude of AB peak is ∼3 % w.r.t. background counts) confirms the presence of stacked type-II QDs in the sample as explained above. The inset of Figure 3 shows integrated PL intensity as a function of excitation intensity at $B = 0$ T. The data are fitted (shown by dashed lines) to the $I_{PL} = I_{exc}^{k}$ law [25]. The dependence is almost linear ($k \sim 0.91$) over four orders of magnitude. This is possible if only relatively few QDs are occupied by holes, which supports the assumption of the governing model.

### 3.2.2 Spectral analysis: multiple QDs stacks

The AB oscillation in PL intensity has been most commonly reported in terms of integrated PL intensity [6,9,11,17], which can be seen as an overall averaged interpretation about the QD or QR ensemble. We, however, study the evolution of the AB oscillation, specifically the value of $B_{AB}$, at spectral energies across the PL spectrum. The observed value of $B_{AB}$ determines the characteristic radius of electronic orbit [4]. For $|L = 0\rangle$ to $|L \neq 0\rangle$ transition occurs at such a field that

$$\pi R_e^2 B_{AB} = \Phi_0/2, \qquad (1)$$

where $\Phi_0 = h/e$ is the flux quantum, $R_e$ is the electronic orbit, $h$ and $e$ are the Planck's constant and the electron charge, respectively. Hence, by measuring the $B_{AB}$ across

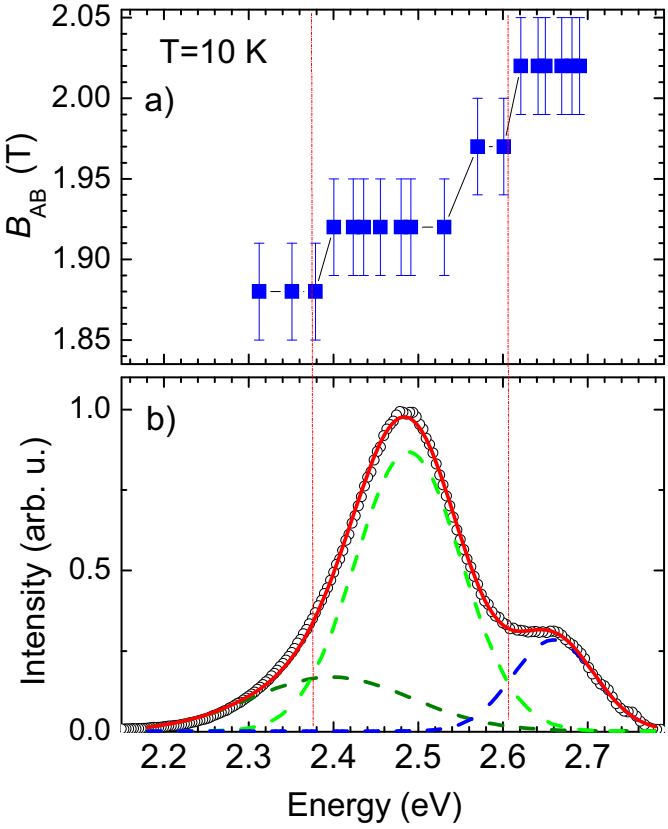


**Fig. 4.** (Color online) a) Variation of $B_{AB}$ as a function of the PL energy across the spectrum shown in b); b) PL spectrum obtained under magneto-PL excitation conditions, decomposed into two "green" and one "blue" band.

the spectra, the lateral spatial component of the exciton wavefunction can be determined with high accuracy [26].

Figures 4a and 4b show the spectral analysis of AB oscillations in intensity from low-temperature (10 K) magneto-PL. The spectral behavior of $B_{AB}$ (Fig. 4a) is shown to relate to the PL spectra (in magneto-PL conditions) shown in Figure 4b. The value of $B_{AB}$ changes from 1.88 T (below ∼2.37 eV) up to 2.02 T (above ∼2.62 eV) and the variations are measurable beyond the experimental error. The size of type-II excitons can be determined (using Eq. (1)) from observed values of $B_{AB}$ for different QD stacks. The excitonic size ranges from 18.7 to 18.0 nm, for the lowest and highest obtained values of $B_{AB}$, respectively. The presence of different sets of QDs stacks is clearly distinguishable within the region of transitions in $B_{AB}$. The PL spectrum (Fig. 4b) is thus decomposed into three Gaussian peaks. Three peaks were used to include the contributions from the two "green" bands (the lower energy green band at ∼2.40 eV, the higher energy green band at ∼2.49 eV), and a "blue" band ∼2.66 eV with "reduced" overlap in the spectral region where the $B_{AB}$ changes its value, for the changes in $B_{AB}$ are observable due to the subdued emission from the overlapping bands in the PL. This allows one to discern the presence of different QDs stacks in the sample. It is thus evident that different sets of QDs stacks are

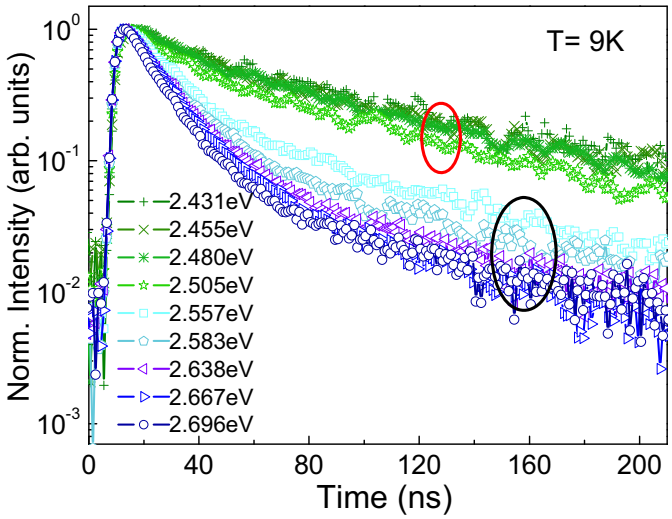


**Fig. 5.** (Color online) TRPL showing "bundling" of decay curves in "green" and "blue" spectral regions.

dominant at specific spectral regions. We suggest that different QD thickness and/or chemical composition rather than lateral size, determine the difference in the PL peak energy between the stacks. This energy, ∼90 meV, is estimated from the peaks of the two Gaussians used to form the green band (Fig. 4b). Such a large difference is unattainable by any realistic change in the QD radius. Indeed, the energy of the hole confinement energy inside a disk-like dot of radius $a$ and thickness $d$ can be estimated as

$$E = \frac{\hbar^2}{2m_h^*}\left[x_{ms}^2 + \frac{n_z^2\pi^2}{d^2}\right], \qquad (2)$$

where $m_h^*$ is the effective mass of hole in ZnTe and $x_{ms}$ are the solutions for $\frac{J_1(x_{ms})}{J_0(x_{ms})} = \frac{N_1(x_{ms})}{N_0(x_{ms})}$. Here $J(x_{ms})$ and $N(x_{ms})$ are the Bessel functions of the first and the second kind, respectively; taken for $m = 0$ and $s = 1$. For the ground state $n_z = 1$ and with realistic values of dot radii ∼9 to 11 nm [6,17,26], $d = 1$ nm [6] the energy is observed to change by only ∼0.1 to 0.2 meV.

### 3.3 Time-resolved PL studies

Further confirmation of distinguishability of QDs stacks within the ensemble system is obtained from TRPL measurements. The time decay curves at various spectral positions across the PL spectrum are shown in Figure 5. A slower decay for lower energy side is observed as was also seen previously [19,23], indicating dominance of "larger" dots on lower energy side and 'smaller' dots and/or IC dominant transitions on higher energy side. Moreover, the PL emission decay curves exhibit a "bundling" at the spectral regions of the green band (below 2.51 eV) and blue band (above 2.58 eV). We note that the decay curve "bundles" are observed at spectral positions for which the $B_{AB}$ values (as observed from spectral analysis of magneto-PL results) remained constant (e.g. between ∼2.4 to 2.5 eV and for ∼2.6 eV and above). We also suggest that initial decay is due to "faster" dots, and the tail is dominated by "slower" dots contributing via "overlap". As the lifetime of radiative recombination depends on the overlap of electron and hole wavefunctions (the larger the overlap, the faster is the decay), such an observation is a direct consequence of the presence of different QDs stacks with distinctive overlap of the wavefunctions, which is dependent on the lateral size of type-II excitons.

In summary, we gained capability of fine probing lateral size of type-II excitons in stacked type-II ZnTe/ZnSe QD system via a spectral study of the AB oscillations in PL intensity. High resolution low temperature cw-PL, magneto-PL and TRPL studies were performed. The spectral analysis revealed a changing AB transition magnetic field, clearly indicating dominance of different stacks of QDs for different emission energies across the PL spectrum. Time-resolved PL confirmed such conclusions. Such fine probing of excitonic characteristics via robust AB oscillations in type-II systems can lead to significant understanding which will be useful towards sustaining applications based on control of exciton-light interaction.

This work is supported by the National Science Foundation under Award No. DMR-1006050. The samples used in this study are grown under Department of Energy, Basic Energy Sciences Grant No. DE-FG02-10ER46678. The authors are thankful to Dr. U. Manna and Profs. L. Mourokh and I.C. Noyan for helpful discussions and support.

## References

1. Y. Aharonov, D. Bohm, Phys. Rev. **115**, 485 (1959)
2. M.V. Berry, Proc. R. Soc. Lond. **392**, 45 (1984)
3. A.B. Kalametsev, V.M. Kovalev, A.O. Govorov, JETP Lett. **68**, 669 (1998)
4. A.O. Govorov, S.E. Ulloa, K. Karrai, R.J. Warburton, Phys. Rev. B **66**, 081309 (2002)
5. M. Bayer, M. Korkusinski, P. Hawrylak, T. Gutbrod, M. Michel, A. Forchel, Phys. Rev. Lett. **90**, 186801 (2003)
6. I.L. Kuskovsky, W. MacDonald, A.O. Govorov, L. Muroukh, X. Wei, M.C. Tamargo, M. Tadic, F.M. Peeters, Phys. Rev. B **76** 035342 (2007)
7. E. Ribeiro, A.O. Govorov, W. Carvalho Jr, G. Medeiros-Ribeiro, Phys. Rev. Lett. **92**, 126402 (2004)
8. A.M. Fischer, J.V.L. Campo, M.E. Portnoi, R.A. Romer, Phys. Rev. Lett. **102**, 096405 (2009)
9. M.D. Teodoro, V.L. Campo, V. Lopez-Richard, E. Marega, G. E. Marques, Y.G. Gobato, F. Iikawa, M.J.S.P. Brasil, Z.Y. AbuWaar, V.G. Dorogan, Y.I. Mazur, M. Benamara, G.J. Salamo, Phys. Rev. Lett. **104**, 086401 (2010)
10. I.R. Sellers, V.R. Whiteside, A.O. Govorov, W.C. Fan, W. C. Chou, I. Khan, A. Petrou, B.D. McCombe, Phys. Rev. B **77**, 241302 (2008)
11. M.H. Degani, M.Z. Maialle, G. Medeiros-Ribeiro, E. Ribeiro, Phys. Rev. B **78**, 075322 (2008)
12. B. Li, F.M. Peeters, Phys. Rev. B **83**, 115448 (2011)
13. A.V. Maslov, D.S. Citrin, Phys. Rev. B **67**, 121304 (2003)

14. F. Palmero, J. Dorignac, J.C. Eilbeck, R.A. Römer, Phys. Rev. B **72**, 075343 (2005)
15. V.M. Fomin, V.N. Gladilin, S.N. Klimin, J.T. Devreese, N.A.J.M. Kleemans, P.M. Koenraad, Phys. Rev. B **76**, 235320 (2007)
16. K.L. Janssens, B. Partoens, F.M. Peeters, Phys. Rev. B **69**, 235320 (2004)
17. I.R. Sellers, V.R. Whitesides, I.L. Kuskovsky, A.O. Govorov, B.D. McCombe, Phys. Rev. Lett. **100**, 136405 (2008)
18. I.L. Kuskovsky, C. Tian, G.F. Neumark, J.E. Spanier, I. P. Herman, W.C. Lin, S.P. Guo, M.C. Tamargo, Phys. Rev. B **63**, 155205 (2001)
19. B. Roy, A. Shen, M. Tamargo, I. Kuskovsky, J. Electron. Mater. **40**, 1775 (2011)
20. Y. Gu, I.L. Kuskovsky, M. van der Voort, G.F. Neumark, X. Zhou, M.C. Tamargo, Phys. Rev. B **71**, 045340 (2005)
21. I.L. Kuskovsky, Y. Gu, M. van der Voort, G.F. Neumark, X. Zhou, M. Munoz, M.C. Tamargo, Phys. Stat. Sol. (b) **241**, 527 (2004)
22. I.L. Kuskovsky, C. Tian, C. Sudbrack, G.F. Neumark, S.P. Guo, M.C. Tamargo, J. Cryst. Growth **214**, 335 (2000)
23. M.C.K. Cheung, A.N. Cartwright, I.R. Sellers, B.D. McCombe, I.L. Kuskovsky, Appl. Phys. Lett. **92**, 032106 (2008)
24. K.L. Janssens, B. Partoens, F.M. Peeters, Phys. Rev. B **64**, 155324 (2001)
25. T. Schmidt, K. Lischka, W. Zulehner, Phys. Rev. B **45**, 8989 (1992)
26. B. Roy, H. Ji, S. Dhomkar, F.J. Cadieu, L. Peng, R. Moug, M.C. Tamargo, I.L. Kuskovsky, Appl. Phys. Lett. **100**, 213114 (2012)